

Analysis of Fiber Attrition and Mechanical Performance in Large-Format Additive Manufacturing of Long-Fiber Reinforced Polymer Composites

Andrew Rhodes¹, Tyler Smith^{1,2}, Christian Sharpe¹, Vlastimil Kunc², Chad Duty^{1,2}

¹ Mechanical, Aerospace, and Biomedical Engineering, University of Tennessee, Knoxville, TN

² Manufacturing Science Division, Oak Ridge National Laboratory, Knoxville, TN

Abstract

Understanding the residual fiber length of discontinuous fiber-reinforced thermoplastics in large-format additive manufacturing (LFAM) is of significant interest since the residual fiber length influences the mechanical properties of the final part. Currently, the attrition of long fiber reinforcement during screw-extrusion LFAM is an understudied subject, although the residual fiber length is among the most important microstructural properties of fiber-reinforced composites. A contributing factor the lack of focus in this area is the questionability and variety of convoluted fiber measurement methods. This study evaluates the relationship between printing speed, the final fiber length, and resultant mechanical properties for 4 mm pultruded thermoplastic polyurethane (TPU) pelletized feedstock and seeks to fully document a fiber length distribution (FLD) measurement method. Samples were printed at several processing speeds and subjected to fiber length analysis and tensile testing. Fiber length analysis was performed using a combination of novel and proven techniques for improved repeatability and reliability of results. This study seeks to improve understanding in the choice of machine design, material selection, and processing parameters for optimal mechanical properties.

Introduction

Background

The use of reinforcing fiber is essential to large-format polymer additive manufacturing [1]. However, the length of the reinforcing fibers is significantly altered through the extrusion process, and the extent of this alteration pertaining to the processing parameters is not well understood, and this process-induced degradation of the fibrous microstructure can induce a noticeable reduction in mechanical properties.

LFAM systems use a single screw plasticating extruder to rapidly deposit large quantities of pelletized material in the printing process. One of the major challenges in printing material this way is the process-induced fiber length reduction. Screw-induced plastication is a high shear process, subjecting the fibers to high stresses that bend and eventually break the fibers [2–8]. Fortunately, this process is near identical to injection molding, where there have been numerous investigations concerning the influence of processing conditions of fiber reinforced plastics, and the resulting mechanical properties of the material. Wolf et al. demonstrated that conditions which increase shear decrease average fiber length [3]. Wolf took fiber length distributions from different regions within the extruder under varying screw speed, temperature, and die diameter. Wolf found that by varying processing conditions to reduce shear (slow screw speed, higher extrusion temperature, larger die diameter) fiber length attrition is reduced. Turkovitch et al. studied the progression of fiber degradation through the length of the extruder and at different screw speeds.

Turkovitch found that fiber degradation advances during extrusion and with screw speed [9]. Yilmazer et al. examined the effects of processing conditions on fiber length and strength in injection molded samples. They reported that fiber length and tensile properties significantly decrease as shear rate is increased by modifying the screw speed and feed rate [8]. Hausnerova et al. studied fiber degradation during multiple extrusion cycles under a range of shear rates through a capillary rheometer. Hausnerova reported that high shear rates degrades fiber length, with significant damage occurring during the first extrusion cycle [10]. In summary, processing conditions have been found to affect mechanical properties through reduction or retention of the initial fiber length distribution, and all these studies rely on accurate fiber length distribution measurement.

Quantifying the residual fiber length distribution is of critical importance in studying the effects of the processing parameters, which directly influence shear and thus the residual fiber length. Additionally, accurate and reliable fiber length distribution (FLD) data are necessary to develop automated measurement tools and predictive models for fiber attrition and mechanical properties. Despite its importance, there is a lack of a defined standard, resulting in a wide variety of incomparable fiber measurement and acquisition methods that exist within academia [11]

This work examines the influence of screw speed on the fiber length of a long fiber material, and tensile properties using a large-format polymer additive manufacturing system. This subject has been extensively studied in an injection molding setting, but it has not been well tested in a screw-extrusion additive manufacturing system like the Cincinnati Big Area Additive Manufacturing (BAAM) used in this study. This study was designed considering that the BAAM extruder is akin to an injection molding extruder, and therefore the effect of processing conditions on fiber length and mechanical properties should follow those of the studies done in injection molding. Additionally, this work examines novel techniques underutilized in FLD measurement and presents improvements to these methods.

Methods

Printed Samples

The material used in this study was pultruded 40% wt. glass fiber thermoplastic polyurethane (TPU). The pellets were of a 4 mm nominal length, but some were found to be a few dozen microns longer (~4.2 mm). The pellets were dried at 80°C for at least 4 hours to remove moisture before printing. The processing parameter varied during this study was screw speed. All other conditions were held constant. The screw speeds tested were 40, 75, and 150 RPM, as this is the range at which the BAAM can successfully print this material. Samples were printed at 230 °C with an 8.89 mm (0.35 inch) diameter nozzle, 7.62 mm (0.3 inch) layer height, and a 17.78 mm (0.7 inch) bead width. Each sample set was printed as a 305 mm (12 inch) x 305 mm (12 inch) x 15.24 mm (0.6 inch) plaque, and then cut to 11.5 inches to closely fit the 11.5-inch square compression mold. The plaques were compression molded at 145 °C under 5 tons for 5 minutes each. The average final thickness for the compressed plaques was 6.5 mm

Tensile specimens (ASTM D638 Type 1) were waterjet cut from the plaques such that the loading direction was parallel to the printed layers or deposition direction [12]. The samples were dried at 50 °C for least 48 hours and left in a desiccant chamber at 23°C for 12 hours (ASTM D618-B) prior to tensile testing. Specimens that incurred damage prior to testing were discarded.

Tensile testing of all specimens was performed on an MTS Criterion Series, Model 45 with a 10kN load cell. The testing rate of 5 mm/min was used for a nominal strain rate of 0.5 mm/(mm min). Extension was measured using an MTS LX 500 Laser Extensometer. Specimens that fractured outside of the gage length were omitted from the data analysis. To ensure statistical significance a minimum of 5 specimens were measured for each condition.

Fiber Length Analysis Method and Techniques

The objective of the FLD measurement process is to obtain a distribution that characterizes the microstructure of the composite and can be divided into seven steps. FLD measurement is performed by firstly isolating a small, manageable portion of the composite called a coupon. Second, the matrix material is removed, often by pyrolysis. Third, a subset of the fibers is selected for measurement through a process called down-sampling. Fourth, the fibers are dispersed and prepared for image capture. Fifth, a digital image is created via microscopy or a document scanner. Sixth, the image is measured either by hand or machine using an image processing software. Seventh, the data is analyzed, and potential biases induced by the prior steps are considered and amended. In the following pages, the specific FLD methods and techniques used in this study will be explained and discussed.

1. Composite coupon extraction

To accurately characterize the fiber length distribution within the polymer matrix, coupons of the printed composites were cut material via a 1.25-inch interior diameter hole saw with the guide bit removed [Figure 1]. According to Kunc et al., the coupon size should at least be twice as large as the longest possible fiber, so that fibers cut during the couponing step can be excluded from measurement simply by extracting fiber from the center of the sample [13]. Future experiments complementary to this study were planned to include a maximum of 12 mm fiber, and so a hole saw with a diameter greater than twice that length (31.75 mm or 1.25 inch) was selected to sample the coupons. A circular coupon is preferable to a rectangular one for the speed and consistency at which samples can be taken. A consistently sized coupon is required so that it closely fits its constraining container during the matrix removal step.

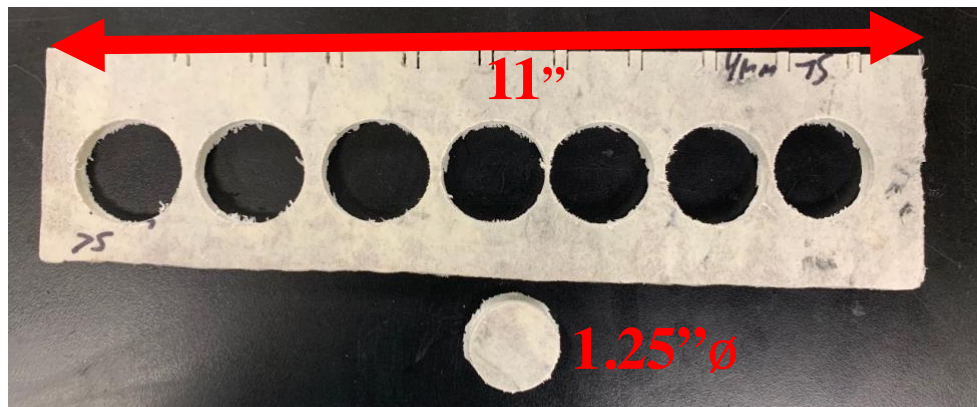


Figure 1: Composite coupon and the plank from which it was cut

2. Constrained removal of matrix material

The composite coupon is placed in a 1.25-inch interior diameter aluminum pipe as the constraining vessel for pyrolyzation or burn-off of the TPU matrix material [Figure 2]. The bottom of the pipe was covered with aluminum foil and attached loosely via a steel hose clamp to keep the foil bottom secure. The top was left open during burn-off. Constraint of the sample is necessary to roughly preserve the structure of the sample during the expansion of the matrix material and release of elastic energy stored in the fiber during when they were extruded. Unconstrained burn-off can result in a pile or puff of fiber, rather than a stack. The top of the sample is left unconstrained to allow for gas to escape, as well as to allow the sample to expand vertically. Burn-off was performed in-air for 4 hours at 500°C with a heat ramp of 3°C/min using a small crucible oven. Some sources reported successful pyrolyzation for 2 hours at 400°C, but that left significant char on the fibers.



Figure 2: Constraining container and the composite coupon fiber stack

3. Fiber sample isolation / down sampling

The fiber sample isolation step involves isolating a portion of fibers from the coupon which represent the FLD of the composite while excluding the damaged fibers near the coupon's edge. This was performed with the epoxy plug method developed by Kunc et al.[13]. This method involved inserting a 22-gauge hypodermic needle attached to a 1 milliliter syringe loaded with an epoxy resin through the center of the coupon and retracting the needle while dispensing epoxy at a continuous rate, resulting in a cylindrical column of epoxy resin that encapsulates fibers within the center of the coupon fiber stack. A Bondic UV curing resin was used since glass fiber can refract the UV light, resulting in significantly faster cures than with an epoxy resin. A 3D printed disk with a center hole for the needle was used as the lid to ensure central alignment of the needle, as well as to lightly compress the fiber to prevent them from sticking to and rising as the needle retracts. The needle was inserted through the entirety of the coupon, such that the needle tip is protruding from the bottom of the aluminum foil bottom. The resin injection was conducted using a custom designed & built actuator for precise control of the needle withdrawal rate and the

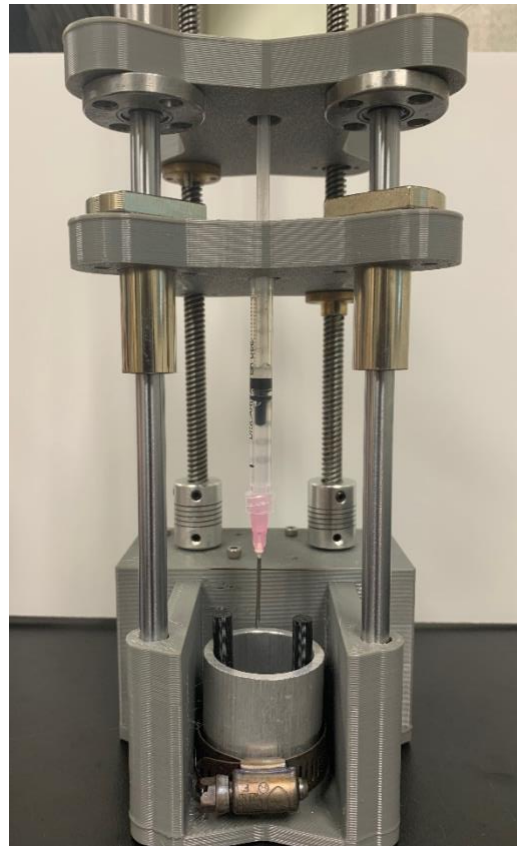


Figure 3: Epoxy depositor

volume of resin deposited [Figure 3]. The depositor is composed of common 3D printer components (Nema 17 motors, TMC2209 stepper drivers, LM8UU bearings, etc.), and an Arduino. Two independently addressable stages allow for precise customization of the resin column size. After the epoxy was deposited, a 5-watt UV flashlight was aimed at the top of the sample for approximately 30 seconds, and at the bottom hole for 30 more seconds, after which the resin would be cured enough to remove the sample from the container. Removal of the sample was performed by sliding the hose clamp off and loosening the sides of the aluminum foil bottom from the container. Then, the 3D printed disk lid was carefully held down while lifting the container up, resulting in the removal of the fiber stack from the container. The UV light was shone on the fiber stack from the cardinal angles for 30 seconds each to aid in a more consistent cure as the samples in this study were highly fiber dense (40 weight percent). In the future, use of a stronger UV lamp would likely improve penetration of the light through the fiber stack to decrease cure time. Additionally, it is useful to add a small amount of epoxy to the top of the plug to act as a handle. The epoxy-bound fibers are extracted by grabbing an edge of the plug with tweezers and using a small, soft paint brush to shed uncaptured fiber from the plug.

Once the plugged fibers are isolated, burn-off of the resin is performed using the same program as the first burn-off, but with the maximum temperature time set to two hours. During this burn-off, the fibers are partially disentangled via the expansion of the resin. The heat ramp of 3°C/min was sufficient for this study, but slower heat ramps can improve disentanglement [11].

4. Filament dispersion

A well dispersed image is important in several senses. Firstly, images can potentially contain tens of thousands of fibers, and it is unreasonable and impractical for a human to measure each one. If a fiber field is evenly dispersed, a human operator can take a subsection or subsections of the image that contains the number of fibers needed, while being fairly confident that the fibers measured are statistically representative of the entire fiber distribution. Secondly, the elimination of fiber bundles or areas of highly dense fiber and overlaps is important for measuring the distribution by hand, through one of the few free but difficult to use automated methods, or inaccessible proprietary options for automatic fiber length measurement [11,14–16].

Initial experiments with fiber dispersion methods showed inconsistency and potential breakage of fiber. These included mechanical means like brushing [13,15], submersion and manual mixing in liquid [14], and ultrasound [17].

It was found that a novel method introduced by Goris et al. provided a low-input, non-mechanical solution to disentangle loose fiber bundles and evenly disperse fiber upon the glass sheet of an image scanner [11]. Under this method, the fibers are dispersed within an enclosed funnel/chamber system using gentle bursts of compressed air. The turbulence causes fibers to disentangle and disperse evenly. A can of compressed air was used with light pressure on the trigger and was found to sufficiently disperse the fiber. Since there is potential for the air pressure to be too great and blow fiber back towards the user, some care is required to lightly release air from the can, and it is recommended to add several inches of space between the mouth of the funnel and the nozzle of the air canister, or apply a seal to the mouth of the funnel and air canister nozzle. The pressurized air from the small

canister nozzle will push a larger wall of air, which is strong enough to disperse the fibers, but gentle and enough to prevent fibers from blowing back. A detailed schematic of the dispersion funnel is shown in Figure 4. The funnel was reverse engineered using Goris's drawings of their funnel, and 3D printed. The funnel was sketched over the original and designed to fit the image scanner used in this study. It should be noted that Goris used polished stainless steel and a dry graphite lubricant to prevent fibers from sticking to the surface of the funnel, but in the current trials, no fiber could be found stuck to the walls of the printed funnel via inspection, and so the unprocessed printed funnel was deemed sufficient. Additionally, it is important to ensure that the funnel is sealed well where it meets the scanner. Failure to do so will result in air traveling out the gaps, resulting in a higher concentration of fiber near the gaps.

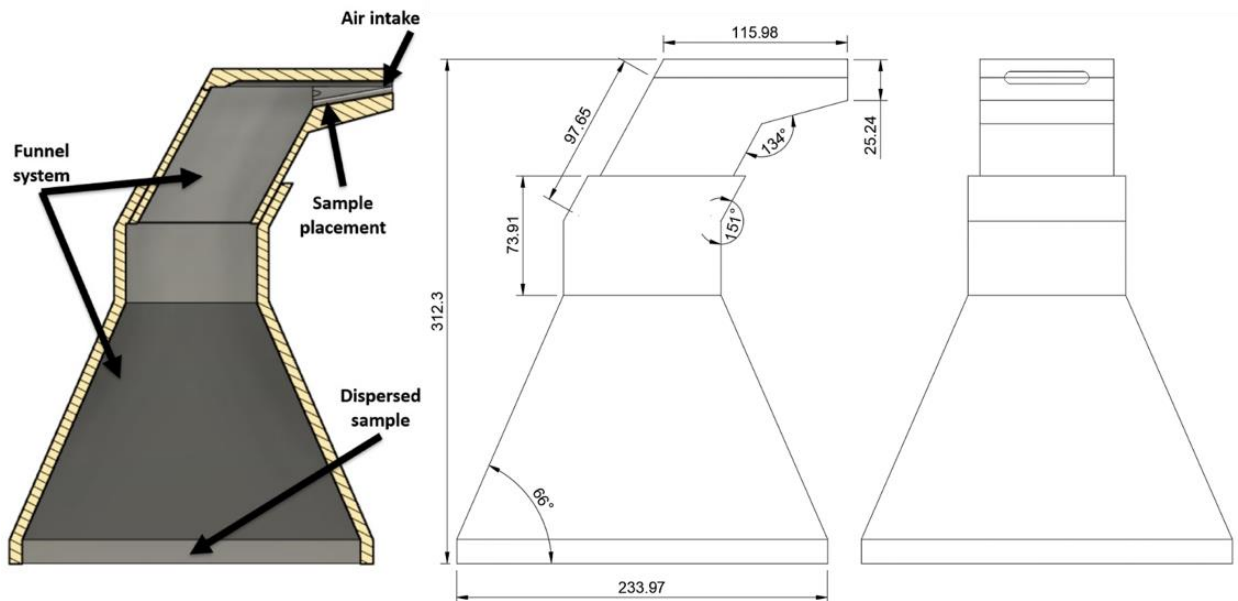


Figure 4: CAD drawing of the fiber dispersion funnel

5. Image capture

Imaging was performed on a Canon CanoScan LiDE 400 at 2400 dpi. The plastic back plate was painted a matte black to provide a higher contrast for the fiber. Huntz brand A4 sized, 4 mm thick, self-adhesive plastic laminating sheets were laid sticky-side up on the scanner before fiber dispersion. This held fibers in place where they fell, ensuring none could be scattered by air in the lab, and allowed for the rapid swapping of samples. Glass panes totaling about 1/4 inch thick were placed on top of the fibers to sandwich them in place against the scanner bed, and to bring the background out of focus, which may have small scratches in the paint that could be mistaken as fiber. In addition, the thickness of the glass panes further separated the scanner surface from the back plate, which seemed to enhance the visibility of the fibers, perhaps by allowing the glass filament to reflect the light from the scanner bar. Similar results were seen by scanning with the back plate open and a dark box covering the scanner. An example scanned image can be seen in **Figure 5**.

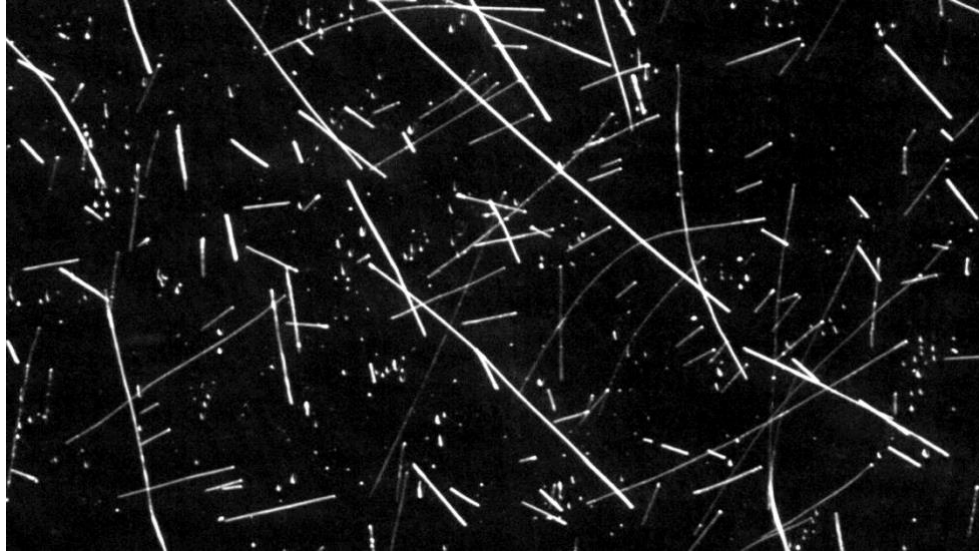


Figure 5: Scanned image example with enhanced contrast for clarity. The duller fibers are out of plane to some degree; probably stacked upon the brighter fibers.

6. Fiber length measurement

The scanned images were processed and hand-measured using ImageJ [18]. To ensure the measured distribution was statistically representative, a minimum of 2000 fibers were measured per sample, as specified in ISO:22314, although the distribution seemed to begin to stabilize at around 500 fibers [19].

Ideally, the entire image would need to be measured to obtain a truly representative distribution. However, this is not practical to do by hand, as a single epoxy plug can potentially contain several tens of thousands of fibers. To reduce bias induced by measuring a smaller number of fibers, images are divided into gridded subsections by multiples of the original fiber length. 45 times the square of the original length (4 mm) was chosen as the grid size (720 mm²), which contained on average 600 – 800 fiber per grid. Assuming that the spatial distribution of all fibers was uniform due to the funnel system used in step 4, any gridded subsect should contain a representative length distribution. To remove potential bias induced by sampling fibers intersecting the grid lines, it was decided that overlaps on the top and left sides would not be measured and overlaps on the bottom and right sides would be measured as shown in Figure 6. This removes the potential to add bias by measuring more long fiber, which are more likely to be measured if crossing a border, and short fiber which are more likely to not cross a border. An added benefit of measuring border overlaps this way is that each border can correspond to a unique grid, so neighboring grid squares can be measured without interfering with shared fibers. In this study, grids squares were measured diagonally from the centermost square to the bottom right of the image.

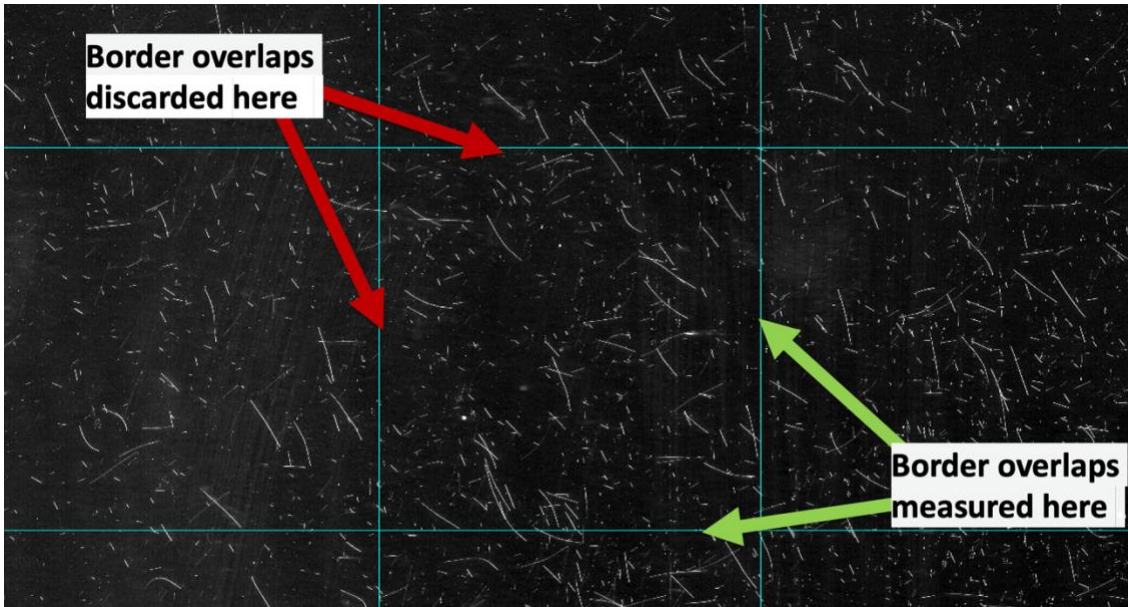


Figure 6: Grided image example showing the border measurement classifications

7. Analysis

Two statistics were used to represent the fiber length distributions: the arithmetic mean and the length-weighted mean.

The arithmetic mean is a representation of the number of shorter fibers, calculated by the sum of the individual fibers divided by the total number of fibers measured. The length-weighted mean is calculated as the sum of the individual fiber lengths squared divided by the sum of the individual fiber lengths. The arithmetic mean is an indicator of the presence of short fibers, and the length-weighted mean gives more importance to longer fibers. Both values are often included in fiber length analyses and are useful in comparing the degree of length reduction of fiber on both sides of the distribution.

$$L_n = \frac{\sum N_i l_i}{\sum N_i} \quad (1)$$

$$L_w = \frac{\sum N_i l_i^2}{\sum N_i l_i} \quad (2)$$

Results and Discussion

Fiber Length Distribution vs. Screw Speed

A summary of the results of the fiber length analysis can be seen in Figure 7 and Table 1. The length data was first validated by measuring the FLD of the 4 mm pultruded pellets. The results show that 62% of the observed fiber are within 0.2 mm of 4 mm, and 29% are 0.2 mm within 0.3 mm. The first condition tested was the 40 RPM screw speed. Considering that the initial fiber length began at 4 mm, the results show that the process of extruding the material is torturous to the fiber. The 40 RPM condition exhibits a bimodal distribution with a high concentration of fibers near the original length and 0.4 mm. Certain theories on fiber breakage mechanisms may explain the large disparity. For example, Mittal et al. and Yilmazer et al. suggest that given the high fiber density of the material used, fiber bundles may survive and protect each other from bending and breaking during extrusion [8,20]. The 75 RPM samples have a similar distribution to the 40 RPM, likely due to the relatively small increase in screw speed. The 150 RPM results show that the longer fiber mode experienced a significant reduction and had the largest body of short fibers of all the samples near the 0.4 mm length. The increase in shear from the 75 RPM condition seems to have overcome any mechanisms preserving the longer fibers in the 40 RPM and 75 RPM conditions.

4 mm Fiber	Arithmetic Mean FL	Weighted Mean FL
Pellets	2.8 mm	3.88 mm
40 RPM	1.36 mm	2.50 mm
75 RPM	1.00 mm	2.27 mm
150 RPM	0.776 mm	2.00 mm

Table 1: Fiber length average representations from the feedstock and tested screw speeds

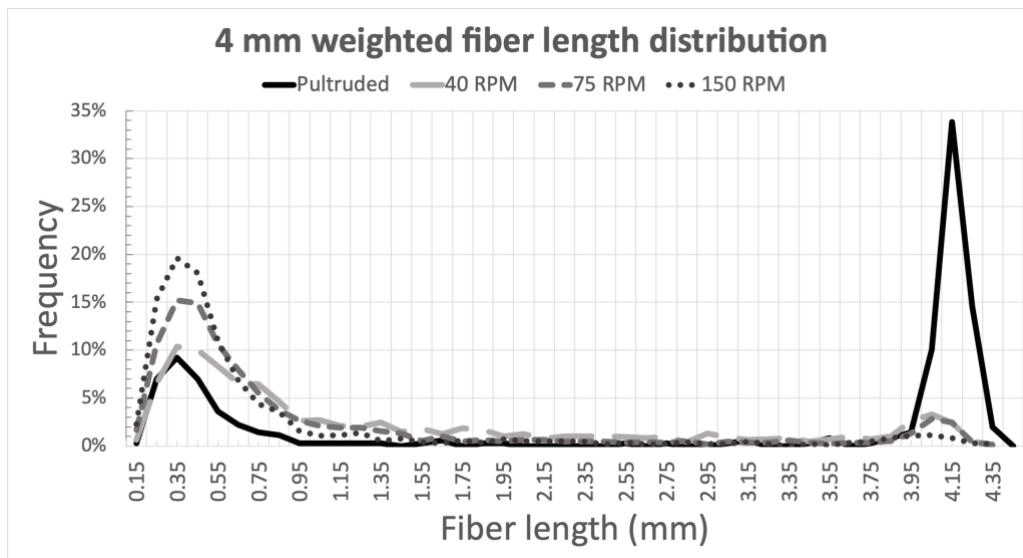


Figure 7: Comparison chart of the fiber length distributions for the 40, 75, and 150 RPM conditions.

Tensile Properties vs. Screw Speed

Figure 8 exhibits the relationship between screw speed on the elastic moduli and ultimate tensile strengths of the tensile specimens respectively. A trend line of the length weighted fiber average is added to the plots to compare the relationship between the average fiber length and tensile properties. As expected, the results show that mechanical performance decreases with shorter fiber length. For the meager difference in fiber length between the 40 RPM and 75 RPM conditions, the tensile properties are roughly equivalent to each other. In the 150 RPM condition, doubling the RPM from 75 resulted in a decrease of about 0.5 mm in both metrics for average fiber length, and a reduction in modulus and strength by about half. It is interesting to note that 150 RPM is near the upper limit of what is a reasonable speed for the BAAM system. Printing at higher speeds would approach the motor's maximum torque where incomplete melting and a general reduction in print quality would be seen.

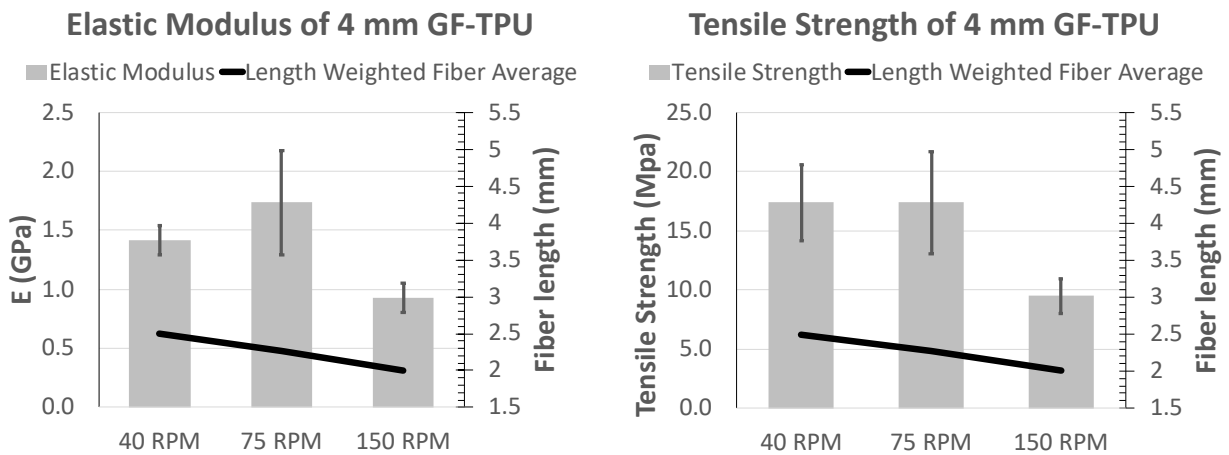


Figure 8: Elastic modulus and ultimate tensile strength of the 4 mm initial fiber length GF-TPU plotted with the respective length-weighted mean fiber lengths

Conclusions

Through extensive experimentation and consolidation of similar studies, a comprehensive method for successfully extracting and measuring the fiber length distributions of long fiber composite materials was fully documented and verified, providing one of the first step-by-step procedures in the field. Screw speed was found to have a meaningful effect on the fiber length and mechanical properties of fiber reinforced large-format printed material under the conditions of this experiment. It was seen that lower screw speeds did not significantly affect fiber attrition; however, there is an inflection point at which the influence of screw speed increases. Further investigations that vary initial fiber length and screw speeds will help to identify whether there is a fiber length retention zone in which screw speed does not significantly affect fiber attrition and how it relates to the inflection point. This will provide an analog for the degree of fiber length attrition common in large-format additive manufacturing for the GF-TPU material used here and in similar composite feedstocks. Further work aims to implement deep learning to create a fiber length analysis network capable of measuring the entirety of an epoxy plug's FLD, cementing the validity of the fiber measurement methods used in this experiment.

Acknowledgements

This research was sponsored by the U.S. Department of Energy, Office of Energy Efficiency and Renewable Energy, Advanced Manufacturing Office, under contract DE-AC05-00OR22725 with UT-Battelle, LLC. This research was also supported by the National Science Foundation under Award No. 2055529.

References

- [1] L.J. Love, V. Kunc, O. Rios, C.E. Duty, A.M. Elliott, B.K. Post, R.J. Smith, C.A. Blue, The importance of carbon fiber to polymer additive manufacturing, *J. Mater. Res.* 29 (2014) 1893–1898. <https://doi.org/10.1557/jmr.2014.212>.
- [2] A. Durin, P. De Micheli, J. Ville, F. Inceoglu, R. Valette, B. Vergnes, A matricial approach of fibre breakage in twin-screw extrusion of glass fibres reinforced thermoplastics, *Compos. Part Appl. Sci. Manuf.* 48 (2013) 47–56. <https://doi.org/10.1016/j.compositesa.2012.12.011>.
- [3] H.J. Wolf, Screw plasticating of discontinuous fiber filled thermoplastic: Mechanisms and prevention of fiber attrition, *Polym. Compos.* 15 (1994) 375–383. <https://doi.org/10.1002/pc.750150508>.
- [4] M. Rohde, A. Ebel, F. Wolff-Fabris, V. Altstädt, Influence of Processing Parameters on the Fiber Length and Impact Properties of Injection Molded Long Glass Fiber Reinforced Polypropylene, *Int. Polym. Process.* 26 (2011) 292–303. <https://doi.org/10.3139/217.2442>.
- [5] B.M. Lekube, B. Purgleitner, K. Renner, C. Burgstaller, Influence of screw configuration and processing temperature on the properties of short glass fiber reinforced polypropylene composites, *Polym. Eng. Sci.* 59 (2019) 1552–1559. <https://doi.org/10.1002/pen.25153>.
- [6] A. Inoue, K. Morita, T. Tanaka, Y. Arao, Y. Sawada, Effect of screw design on fiber breakage and dispersion in injection-molded long glass-fiber-reinforced polypropylene, *J. Compos. Mater.* 49 (2015) 75–84. <https://doi.org/10.1177/0021998313514872>.
- [7] B. Franzén, C. Klason, J. Kubát, T. Kitano, Fibre degradation during processing of short fibre reinforced thermoplastics, *Composites.* 20 (1989) 65–76. [https://doi.org/10.1016/0010-4361\(89\)90684-8](https://doi.org/10.1016/0010-4361(89)90684-8).
- [8] U. Yilmazer, M. Cansever, Effects of processing conditions on the fiber length distribution and mechanical properties of glass fiber reinforced nylon-6, *Polym. Compos.* 23 (2002) 61–71. <https://doi.org/10.1002/pc.10412>.
- [9] R. von Turkovich, L. Erwin, Fiber fracture in reinforced thermoplastic processing, *Polym. Eng. Sci.* 23 (1983) 743–749. <https://doi.org/10.1002/pen.760231309>.
- [10] B. Hausnerova, N. Honkova, A. Lengalova, T. Kitano, P. Saha, Rheology and fiber degradation during shear flow of carbon-fiber-reinforced polypropylenes, *Polym. Sci. Ser. A.* 48 (2006) 951–960. <https://doi.org/10.1134/S0965545X06090100>.
- [11] S. Goris, T. Back, A. Yanev, D. Brands, D. Drummer, T.A. Osswald, A novel fiber length measurement technique for discontinuous fiber-reinforced composites: A comparative study with existing methods, *Polym. Compos.* 39 (2018) 4058–4070. <https://doi.org/10.1002/pc.24466>.
- [12] ASTM D638, (n.d.).
- [13] V. Kunc, B. Frame, N. Nguyen, C.L.T. Iii, G. Velez-Garcia, FIBER LENGTH DISTRIBUTION MEASUREMENT FOR LONG GLASS AND CARBON FIBER REINFORCED INJECTION MOLDED THERMOPLASTICS, (n.d.) 11.

- [14] Home - FASEP Fiber Length Distribution, (n.d.). <http://www.fasep.biz/> (accessed August 19, 2022).
- [15] R. Giusti, F. Zanini, G. Lucchetta, Automatic glass fiber length measurement for discontinuous fiber-reinforced composites, *Compos. Part Appl. Sci. Manuf.* 112 (2018) 263–270. <https://doi.org/10.1016/j.compositesa.2018.06.016>.
- [16] M. Frei, F.E. Kruis, FibeR-CNN: Expanding Mask R-CNN to improve image-based fiber analysis, *Powder Technol.* 377 (2021) 974–991. <https://doi.org/10.1016/j.powtec.2020.08.034>.
- [17] A. Rhodes, R. Walker, T. Smith, J. Lindahl, V. Kunc, C. Duty, Correlating Large-Format AM Print Parameters to Fiber Length and Mechanical Performance of Reinforced Polymer Composites, in: University of Texas at Austin, 2021. <https://doi.org/10.26153/tsw/17601>.
- [18] ImageJ, (n.d.). <https://imagej.nih.gov/ij/> (accessed August 23, 2021).
- [19] 14:00-17:00, ISO 22314:2006, ISO. (n.d.). <https://www.iso.org/cms/render/live/en/sites/isoorg/contents/data/standard/03/61/36185.html> (accessed August 22, 2022).
- [20] R.K. Mittal, V.B. Gupta, P.K. Sharma, Theoretical and experimental study of fibre attrition during extrusion of glass-fibre-reinforced polypropylene, *Compos. Sci. Technol.* 31 (1988) 295–313. [https://doi.org/10.1016/0266-3538\(88\)90035-8](https://doi.org/10.1016/0266-3538(88)90035-8).